 doi:10.20944/preprints202207.0310.v1

Article

Ab-initio Molecular Dynamics Simulation of the Changes in the Optical Properties of 2D MoS_2 When Doped with Pt at 300 K

Juan Manuel Ramírez-de-Arellano [1]*, Ali Fransuani Jiménez-González [2] , Mónica Canales [1] and Luis Fernando Magaña [2,*]

[1] Tecnologico de Monterrey, Escuela de Ingeniería y Ciencias, Calle del Puente #222, Ciudad de México, 14380, México; mcanales@tec.mx (M.C.)
[2] Instituto de Física, Universidad Nacional Autónoma de México, Apartado Postal 20-364, Ciudad de México 01000, México; alifransuanijg@gmail.com (A.F.J-G.)
* Correspondence: jramirezdearellano@tec.mx (J.M.R.-d.-A.); fernando@fisica.unam.mx (L.F.M.)

Abstract: Using first-principles molecular dynamics (FPMD), we performed numerical simulations at 300 K to explore the interaction of a 2D MoS_2 surface and a platinum atom, calculating the optical properties of the resulting material. The pristine MoS_2 is a semiconductor with a gap of around 1.80 eV. The Pt atom is chemisorbed by the surface with an adsorption energy of −1.72 eV. With the adsorption of the Pt atom, the material remains a semiconductor, and its energy band gap reduces to 1.04 eV. But changes in the material's energy band structure imply substantial changes in its optical properties. The energy band structure of the 2D MoS_2 with a sulfur vacancy V_S shows that the material becomes a conductor, and there are significant changes in its optical properties. We also found that the Pt atom chemisorbs in a sulfur vacancy of the material, with an adsorption energy of −4.12 eV. After the adsorption of Pt atoms in the sulfur vacancy, the material becomes a semiconductor with a band gap of 1.06 eV, and the changes in the optical absorption and reflectivity are significant.

Keywords: ab-initio; DFT calculations; 2D materials; MoS_2; optical properties; platinum; FPMD

1. Introduction

Bidimensional materials show different interesting physical properties, making them suitable for many potential applications, including energy storage [1–3], biomedical research [4–6], field-effect transistors (FETs) [7–10], as well as sensors and biosensing [11,12]. One of such materials is Molybdenum disulfide, MoS_2, a layered dichalcogenide with a hexagonal structure similar to graphene. Like graphene, the bonds between layers are weaker, allowing for a relatively easy dislocation [13–16]. Monolayer MoS_2 is also a direct-gap semiconductor with a band gap of 1.8 eV [17] with potential applications that have been explored in fields as diverse as ultrafast photonics, treatment of antibiotic-polluted water, drug-delivery purposes, water splitting, and FETs[18–24].

Studying the band structure and optical properties of such 2D materials helps explore their potential applications. The band structure of MoS_2 has been previously explored, including the effect of interlayer pressure [25]. Here, we studied the changes produced in the optical properties of MoS_2 when adsorbing Pt. We considered pristine MoS_2 and MoS_2 with a sulfur monovacancy (also labeled as Vs) on the unit cell. Vacancies on MoS_2 have been previously studied experimentally and by first-principles calculations, finding relatively low formation energies for a Vs vacancy [16,26], which in turn makes it relatively easy to find.

Preprints (www.preprints.org) | NOT PEER-REVIEWED | Posted: 21 July 2022 doi:10.20944/preprints202207.0310.v1

2. Results

Figure 1(a, b) shows the hexagonal unit cell considered. With a cell parameter of 6.3 Å, it contains 12 atoms: eight S atoms and four Mo atoms. We chose the size of the cell to ensure a sufficiently long distance between one bit and its repetition in the next cell due to the use of periodic boundary conditions. The unit cell we considered is large enough to give a sufficiently good amount of information while avoiding spurious interactions. Starting from this cell, we removed one S atom to create a vacancy. Figure 1(c) shows the PDOS for the pristine MoS_2, with a gap of 1.8 eV, in agreement with previously reported works [25]. Below the Fermi energy, notice the hybridization of orbitals p and d from molybdenum with orbitals s and p from sulfur. Above 2 eV, we can see the hybridization of the same orbitals, but the contribution of orbital p from molybdenum is negligible.

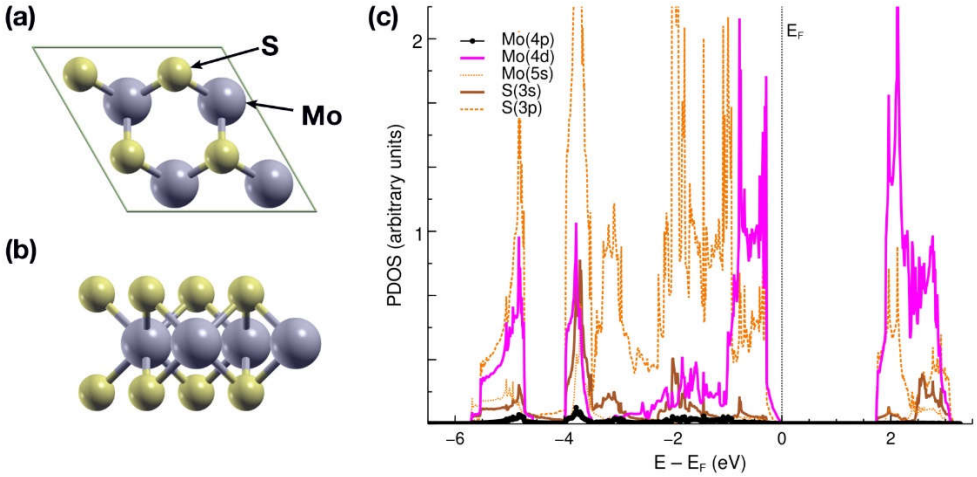

Figure 1. (a) XY-plane view of the unit cell considered for the pristine MoS_2. It contains 12 atoms: four Mo and eight S atoms. The cell parameter is 6.3 Å. (b) XZ-plane view of the unit cell. (c) The PDOS for the pristine MoS_2, showing a gap of 1.8 eV.

2.1. Pt-absorption on the pristine MoS_2 layer

We first placed the Pt atom at 3 Å directly above the MoS_2 surface. The ab-initio molecular dynamics calculation at 300 K showed that the MoS_2 surface absorbed the Pt atom, with an adsorption energy of −1.72 eV. Figure 2(a) shows the initial and final positions of the Pt atom during the adsorption process on the MoS_2 layer, along with a plot of the energy evolution of the system during the calculation. Figure 2(b) offers the PDOS for the Pt atom adsorbed on the pristine MoS_2. The effect of the absorbed Pt atom is a reduction of the band gap, which was observed to be of 1.04 eV in this case. Between 0 and −1.5 eV, there is a hybridization of orbitals s and d from platinum with orbitals s from sulfur and d from molybdenum. Below −6 eV, we have hybridized orbitals s, p, and d from molybdenum with orbitals s and d from platinum. Above 2 eV, we can see the hybridization of the same orbitals, but the contribution of orbital p from molybdenum is again negligible.

Preprints (www.preprints.org) | NOT PEER-REVIEWED | Posted: 21 July 2022 doi:10.20944/preprints202207.0310.v1

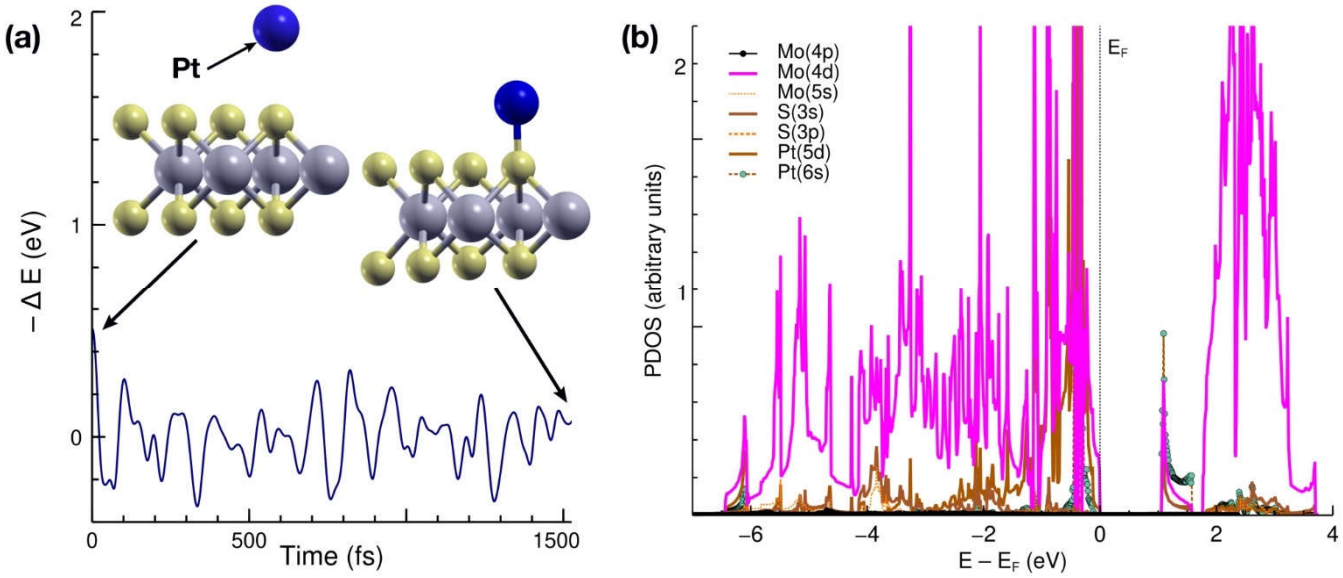

Figure 2. (a) Time evolution graph including the initial and final positions of the Pt atom interacting with the pristine MoS2 surface. The MD calculation consisted of 1526 iterations and the system achieves stability at about 200 fs, much faster than the next case; (b) The PDOS of the system pristine MoS2-Pt. The band gap is reduced to 1.04 eV in this case.

2.2. Pt-absorption on the MoS_2 + V_S vacancy layer

The next case considered was that of a sulfur V_S vacancy in the MoS_2 surface and its interaction with Pt. We performed FPMD calculations at 300 K for an initial configuration with the Pt atom at 3 Å directly above the S-vacancy of the system, like in the previous case (see Figure 3(a)). We obtained that the Pt atom is chemisorbed in the V_S vacancy, with an absorption energy of –4.12 eV. The vacancy we are considering in our unit cell is equivalent to a vacancy density of 12.5% on the surface. Figure 3(b) shows the PDOS for the Pt atom adsorbed on the MoS_2 surface. The band gap for this case was observed to be 1.06 eV. Between 0 eV and −4 eV, we can see the hybridization of the orbitals s and d from platinum with orbitals s and p from sulfur and p and d from molybdenum. Furthermore, between −4 eV and −6 eV, we have the hybridization of orbitals s, p, d from molybdenum with orbitals s, d from platinum and orbitals s, p from sulfur.

Preprints (www.preprints.org) | NOT PEER-REVIEWED | Posted: 21 July 2022 doi:10.20944/preprints202207.0310.v1

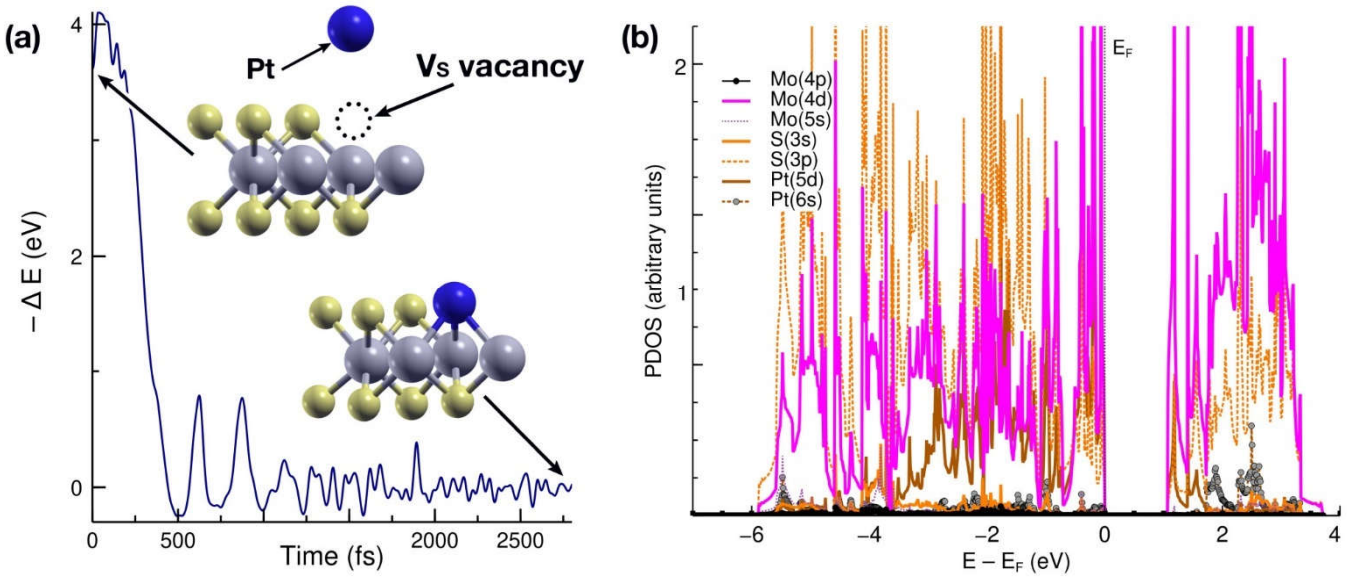

Figure 3. (a) Initial and final configurations during adsorption of a Pt atom on the MoS_2 system with a V_S vacancy. The time evolution graph shows that stability appears after about 700 fs. The MD calculation at 300 K consisted of 2800 iterations and shows that the Pt is chemisorbed by the surface, occupying the place of the vacancy; (B): The PDOS of the final system, showing a reduction similar to that of the previous case (the band gap is now 1.06 eV) when compared with the pristine MoS_2.

2.3. Energy band structures

In Figure 4, we can see the energy band structure calculations for the pristine MoS_2, the same system with an adsorbed Pt atom, the surface with a V_S vacancy, and the latter with an adsorbed Pt atom. The Fermi energy is normalized at zero.

The proposed manipulation of the MoS_2 surface causes an overall reduction in the band gap related to the pristine surface. There are exciting features. Notice that the pristine surface is a semiconductor with a band gap of 1.8 eV, as expected. The adsorption of a Pt atom does not change that property, but it reduces the band gap to 1.04 eV. However, the MoS_2 with a sulfur vacancy becomes a conductor. Furthermore, notice that the adsorption of a Pt atom on the latter destroys the conductor feature, and a band gap appears with a value of 1.06 eV. The changes in the band structure implied substantial changes in the optical properties of the surface.

Preprints (www.preprints.org) | NOT PEER-REVIEWED | Posted: 21 July 2022 doi:10.20944/preprints202207.0310.v1

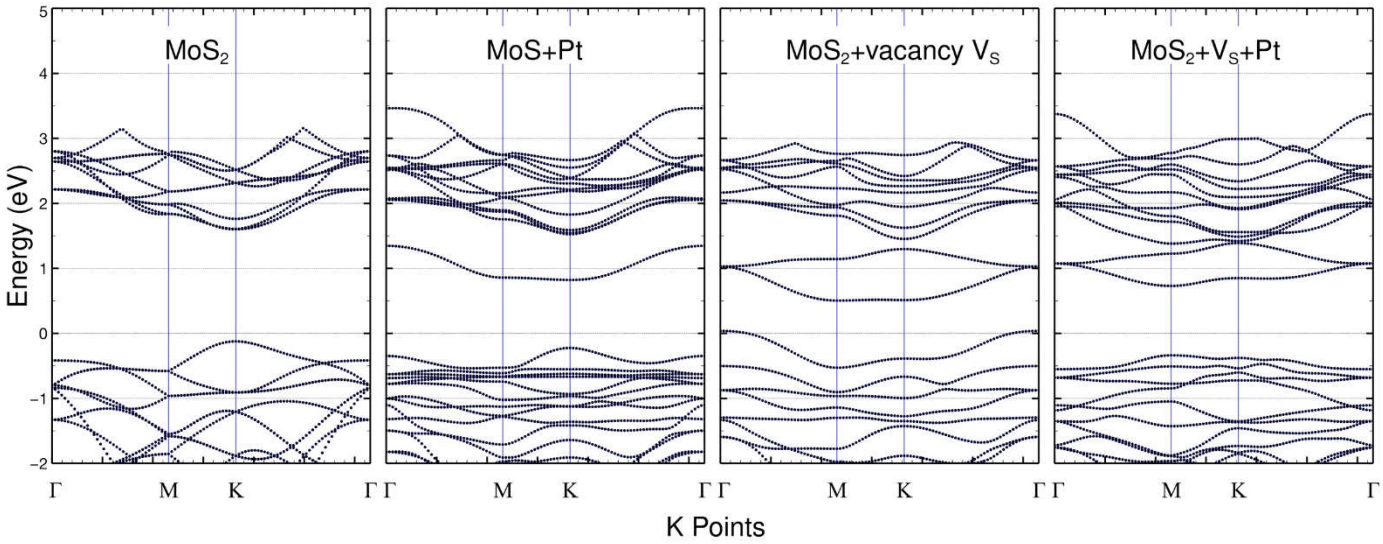

Figure 4. The energy band structure calculations for the pristine MoS_2, the same system with an adsorbed Pt atom, the surface with vacancies, and the latter with an adsorbed Pt atom. The Fermi energy is at zero.

2.4. Optical properties

For each of the cases considered, we calculated the optical absorption spectra in the infrared (IR), visible (VIS), and ultraviolet (UV) range along the Z-axis (see Figure 5). Figure 6 shows the reflectivity.

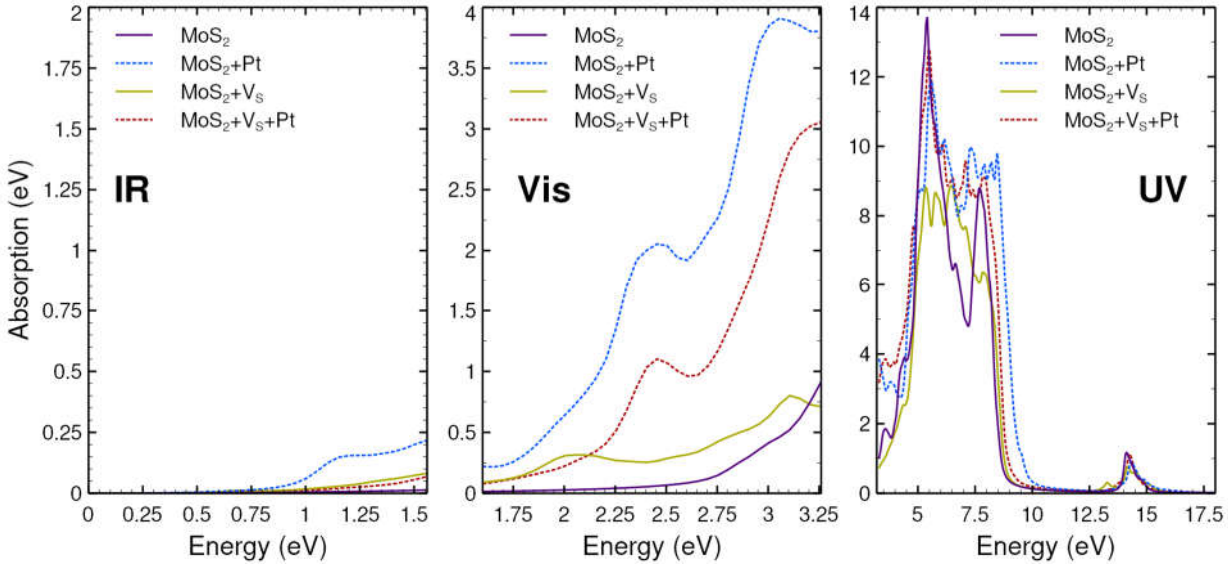

Figure 5. Absorption spectra in the infrared (left), visible (center), and UV (right) ranges, along the direction perpendicular to the surface for the systems we have investigated: pristine MoS_2, Pt adsorbed on pristine MoS_2, the same with a sulfur vacancy (MoS_2+V_S), and the latter surface with a Pt atom adsorbed on the surface (MoS_2+V_S+Pt). The vertical scale is the same for the three sections of the plot, but the range shown differs to make the features of each section more visible. In calculating this graph we have increased numerical precision to guarantee its accuracy.

Notice that the optical absorption in the infrared region has its most significant values for the surface of Pt adsorbed on pristine MoS_2 and the smallest for MoS_2 with a vacancy. We have the same behavior in the visible range, except for the interval between 2.90 eV and 3.25 eV, where the smallest values correspond to MoS_2 with a vacancy. In the ultraviolet region, Pt on the pristine MoS_2 has the most significant absorption, keeping the overall shape related to pristine MoS_2 with about the same positions for peaks and valleys. In this

Preprints (www.preprints.org) | NOT PEER-REVIEWED | Posted: 21 July 2022 doi:10.20944/preprints202207.0310.v1

case, the absorption between 6.00 eV and 7.00 eV is around 46% larger, related to the pristine surface.

In the case of reflectivity, the most substantial change related to pristine MoS_2 is between 0 eV and 5.00 eV and comes from the Pt adsorbed on non-defective MoS_2. In the same region, the smallest values correspond to MoS_2 with a vacancy. The most considerable value for reflectivity is for Pt adsorbed on defective MoS_2, which occurs around 8.6 eV.

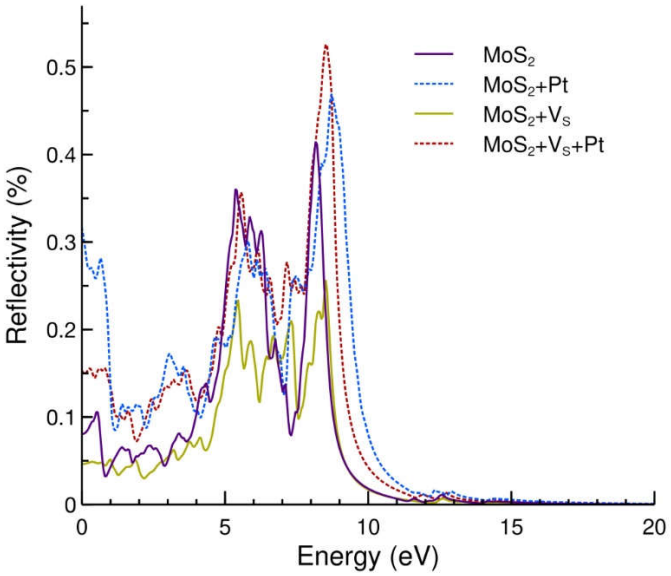

Figure 6. Reflectivity spectra for the three first cases. The substitutionally absorbed Pt atom increases the reflectivity overall. Most of the reflectivity is observed in the visible spectra, with a negligible amount for energies beyond 20 eV.

3. Discussion

We performed FPMD simulations to investigate the Pt adsorption effect on the optical properties of 2D MoS_2. We considered pristine and defective MoS_2 at 300 K and atmospheric pressure. The proposed manipulation of the MoS_2 surface causes an overall reduction in the band gap related to the non-spoiled surface. There are exciting features. The clean surface is found to be a semiconductor with a band gap of 1.8 eV, which agrees with previous works. The adsorption of a Pt atom reduces the band gap to 1.04 eV. However, the MoS_2 with a sulfur vacancy V_S becomes a conductor, as can be seen from the band structure diagram. However, the adsorption of a Pt atom on the latter destroys the conductor feature, and a band gap appears with a value of 1.10 eV. The changes in the band structure implied substantial changes in the optical properties of the surface. Notice that the vacancy we are considering in our unit cell is equivalent to 12.5% vacancy density on the surface.

The optical absorption in the infrared region has its most significant values for the surface of Pt adsorbed on pristine MoS_2 and the smallest for MoS_2 with a vacancy. We have the same behavior in the visible range, except for the interval between 2.90 eV and 3.25 eV, where the smallest values correspond to MoS_2 with a vacancy. In the ultraviolet region, Pt on the pristine MoS_2 has the most significant absorption, keeping the overall shape related to pristine MoS_2 with about the same positions for peaks and valleys. In this case, the absorption between 6.0 eV and 7.0 eV is around 46% larger, related to the clean material.

For the reflectivity, the most substantial change related to pristine MoS_2 is between 0 eV and 5.00 eV and comes from the Pt adsorbed on non-defective MoS_2. In the same region, the smallest values correspond to MoS_2 with a vacancy. The maximum reflectivity is for Pt adsorbed on defective MoS_2, which occurs around 8.60 eV.

Preprints (www.preprints.org) | NOT PEER-REVIEWED | Posted: 21 July 2022 doi:10.20944/preprints202207.0310.v1

Understanding the optical properties of MoS_2 —and the effect that vacancies alone and in combination of the Pt decoration have on them— is essential as it could be helpful in the developing of FETs-related technologies. For future research we are exploring the potential of these combined systems in sensor technologies, particularly for pollutant molecule sensing devices. Another interesting feature reserved for future research is the variation of vacancy concentration and its effects on the properties of these materials.

4. Materials and Methods

All ab-initio calculations in this work were made using the Quantum ESPRESSO code [27,28] within the Density Functional Theory (DFT), the pseudopotential formalism, and the projector-augmented wave (PAW) method [29]. All the calculations were non-relativistic, non-spin polarized, with cut-off energy of 80 Ry (1088 eV), and threshold energy for convergence of 1.0×10^{-6} eV. This code suite considers periodic boundary conditions and plane-wave expansions.

In this work we considered Born-Oppenheimer first principles molecular dynamics (FPMD) as implemented by Quantum ESPRESSO. FPMD is the method chosen whenever bonds may be broken or formed, or in the presence of complex bonding as in transition metals [30–33], which is the case here. The FPMD calculations considered a 551 k-points mesh within the Monkhorst–Pack special k-point scheme [34]. Velocity rescaling (first method) is used to control the temperature of 300 K considered in this work. For the time step, we used the default value of 20.0 a.u. where 1 a.u.= 4.8378×10^{-17} s = 0.048378 fs. This is equivalent to a time step of 0.96756 ≈ 1 fs. The convergence parameter considered for the MD calculations was set as 1.0×10^{-4} eV.

The valence electronic states considered are, for hydrogen: 1s, for molybdenum: $4d^5$ $5s^1$, for sulfur: $3s^2$ $3p^4$, for platinum: $5d^9$ $6s^1$. The geometrical optimizations used an 882 k-points mesh and the stable coordinates obtained from the molecular dynamics. The XCrySDen software was used for visualization purposes [35].

We calculated the energy band structure to obtain the imaginary part of the dielectric tensor. We used the Kramers-Kronig relations [36] to obtain the real part, following the procedure explained in more detail in a previous work [37]. We obtained the reflectivity and the optical absorption by considering the two components of the tensor, using the following equations (where n is the refractive index and k is the extinction coefficient):

$$R_{ii}(\omega) = \frac{(n-1)^2 + k^2}{(n+1)^2 + k^2} \tag{1}$$

$$A_{ii}(\omega) = \frac{2\omega k(\omega)}{c} \tag{2}$$

where

$$n_{ii} = \sqrt{\frac{|\varepsilon_{ii}(\omega)| + \mathrm{Re}\varepsilon_{ii}(\omega)}{2}} \tag{3}$$

$$k_{ii}(\omega) = \sqrt{\frac{|\varepsilon_{ii}(\omega)| - \mathrm{Re}\varepsilon_{ii}(\omega)}{2}} \tag{4}$$

We calculated the adsorption energy for all cases by using the following formula [38]:

$$E_{adsorption} = E_{system\ 1+system\ 2} - E_{system\ 1} - E_{system\ 2} \tag{5}$$

Author Contributions: Conceptualization, J.M.R.-d.-A., and L.F.M.; Data curation, J.M.R.-d.-A. M.C. and A.F.J.G.; Formal analysis, J.M.R.-d.-A. and L.F.M.; Funding acquisition, L.F.M.; Investigation, J.M.R.-d.-A., M.C., A.F.J.G. and L.F.M.; Methodology, J.M.R.-d.-A., A.F.J.G. and L.F.M.; Project

administration, J.M.R.-d.-A., L.F.M.; Resources, L.F.M.; Validation, J.M.R.-d.-A., M.C., A.F.J.G. and L.F.M.; Writing—original draft, J.M.R.-d.-A. and L.F.M.; Writing—review and editing, J.M.R.-d.-A. and L.F.M. All authors have read and agreed to the published version of the manuscript.

Funding: This research was funded by Dirección General de Asuntos del Personal Académico de la Universidad Nacional Autónoma de México, grant number IN113220. The APC was funded by Tecnologico de Monterrey.

Institutional Review Board Statement: Not applicable.

Informed Consent Statement: Not applicable.

Acknowledgments: We thank Dirección General de Asuntos del Personal Académico de la Universidad Nacional Autónoma de México for their partial financial support by Grant IN113220. We also give thanks for UNAM-Miztli-Super-Computing Center's technical assistance by the project LANCAD-UNAM-DGTIC-030. J.M.R.-d.-A. would like to thank Dr. Rolando Pérez Álvarez (UAEM) and Dr. Ernesto Manuel Hernández Cooper (Tecnologico de Monterrey) for their valuable comments regarding this work.

Conflicts of Interest: The authors declare no conflict of interest.

References

1. Arellano, L.G.; De Santiago, F.; Miranda, Á.; Pérez, L.A.; Salazar, F.; Trejo, A.; Nakamura, J.; Cruz-Irisson, M. Ab Initio Study of Hydrogen Storage on Metal-Decorated GeC Monolayers. *International Journal of Hydrogen Energy* **2021**, *46*, 29261–29271, doi:10.1016/j.ijhydene.2021.04.135.
2. Reddy, A.L.M.; Srivastava, A.; Gowda, S.R.; Gullapalli, H.; Dubey, M.; Ajayan, P.M. Synthesis Of Nitrogen-Doped Graphene Films For Lithium Battery Application. *ACS Nano* **2010**, *4*, 6337–6342, doi:10.1021/nn101926g.
3. Moschetto, S.; Bolognesi, M.; Prescimone, F.; Brucale, M.; Mezzi, A.; Ortolani, L.; Caporali, M.; Pingue, P.; Serrano-Ruiz, M.; Pisignano, D.; et al. Large-Area Oxidized Phosphorene Nanoflakes Obtained by Electrospray for Energy-Harvesting Applications. *ACS Appl. Nano Mater.* **2021**, *4*, 3476–3485, doi:10.1021/acsanm.0c03465.
4. Palmieri, V.; Perini, G.; De Spirito, M.; Papi, M. Graphene Oxide Touches Blood: *In Vivo* Interactions of Bio-Coronated 2D Materials. *Nanoscale Horiz.* **2019**, *4*, 273–290, doi:10.1039/C8NH00318A.
5. Donskyi, I.S.; Chen, Y.; Nickl, P.; Guday, G.; Qiao, H.; Achazi, K.; Lippitz, A.; Unger, W.E.S.; Böttcher, C.; Chen, W.; et al. Self-Degrading Graphene Sheets for Tumor Therapy. *Nanoscale* **2020**, *12*, 14222–14229, doi:10.1039/D0NR02159H.
6. Borandeh, S.; Alimardani, V.; Abolmaali, S.S.; Seppälä, J. Graphene Family Nanomaterials in Ocular Applications: Physicochemical Properties and Toxicity. *Chem. Res. Toxicol.* **2021**, *34*, 1386–1402, doi:10.1021/acs.chemrestox.0c00340.
7. Chang, P.; Liu, X.; Liu, F.; Du, G. First-Principles Based Ballistic Transport Simulation of Monolayer and Few-Layer InSe FETs. *Jpn. J. Appl. Phys.* **2019**, *58*, SBBA02, doi:10.7567/1347-4065/aafb4f.
8. Gonzalez-Medina, J.M.; Ruiz, F.G.; Marin, E.G.; Godoy, A.; Gámiz, F. Simulation Study of the Electron Mobility in Few-Layer MoS2 Metal–Insulator-Semiconductor Field-Effect Transistors. *Solid-State Electronics* **2015**, *114*, 30–34, doi:10.1016/j.sse.2015.07.007.
9. Wang, C.; Peng, L.; Wells, S.A.; Cain, J.D.; Huang, Y.-K.; Rhoads, L.A.; Dravid, V.P.; Hersam, M.C.; Grayson, M.A. Field-Effect Conductivity Scaling for Two-Dimensional Materials with Tunable Impurity Density. *2D Mater.* **2022**, *9*, 031002, doi:10.1088/2053-1583/ac72b0.
10. Wu, H.; Cui, Y.; Xu, J.; Yan, Z.; Xie, Z.; Hu, Y.; Zhu, S. Multifunctional Half-Floating-Gate Field-Effect Transistor Based on MoS_2–BN–Graphene van Der Waals Heterostructures. *Nano Lett.* **2022**, *22*, 2328–2333, doi:10.1021/acs.nanolett.1c04737.
11. Sosa, A.N.; Cid, B.J.; Hernández-Hernández, I.J.; Miranda, Á. Effects of Substitutional Doping and Vacancy Formation on the Structural and Electronic Properties of Siligene: A DFT Study. *Materials Letters* **2022**, *307*, 130993, doi:10.1016/j.matlet.2021.130993.
12. Pessanha, T.M.; Paschoalino, W.J.; Deroco, P.B.; Kogikoski, S.; De Moraes, A.C.M.; Carvalho Castro Silva, C.; Kubota, L.T. Interfacial Capacitance of Graphene Oxide Films Electrodes: Fundamental Studies on Electrolytes Interface Aiming (Bio)Sensing Applications. *Electroanalysis* **2022**, *34*, 692–700, doi:10.1002/elan.202100220.

13. Dickinson, R.G.; Pauling, L. THE CRYSTAL STRUCTURE OF MOLYBDENITE. *J. Am. Chem. Soc.* **1923**, *45*, 1466–1471, doi:10.1021/ja01659a020.
14. Schönfeld, B.; Huang, J.J.; Moss, S.C. Anisotropic Mean-Square Displacements (MSD) in Single-Crystals of 2 *H* - and 3 *R* -MoS 2. *Acta Crystallogr B Struct Sci* **1983**, *39*, 404–407, doi:10.1107/S0108768183002645.
15. Gupta, A.; Sakthivel, T.; Seal, S. Recent Development in 2D Materials beyond Graphene. *Progress in Materials Science* **2015**, *73*, 44–126, doi:10.1016/j.pmatsci.2015.02.002.
16. Xiong, Z.; Zhong, L.; Wang, H.; Li, X. Structural Defects, Mechanical Behaviors, and Properties of Two-Dimensional Materials. *Materials* **2021**, *14*, 1192, doi:10.3390/ma14051192.
17. Mak, K.F.; Lee, C.; Hone, J.; Shan, J.; Heinz, T.F. Atomically Thin MoS 2 : A New Direct-Gap Semiconductor. *Phys. Rev. Lett.* **2010**, *105*, 136805, doi:10.1103/PhysRevLett.105.136805.
18. Zhang, H.; Lu, S.B.; Zheng, J.; Du, J.; Wen, S.C.; Tang, D.Y.; Loh, K.P. Molybdenum Disulfide (MoS_2) as a Broadband Saturable Absorber for Ultra-Fast Photonics. *Opt. Express* **2014**, *22*, 7249, doi:10.1364/OE.22.007249.
19. Yin, W.; Yan, L.; Yu, J.; Tian, G.; Zhou, L.; Zheng, X.; Zhang, X.; Yong, Y.; Li, J.; Gu, Z.; et al. High-Throughput Synthesis of Single-Layer MoS 2 Nanosheets as a Near-Infrared Photothermal-Triggered Drug Delivery for Effective Cancer Therapy. *ACS Nano* **2014**, *8*, 6922–6933, doi:10.1021/nn501647j.
20. Liang, W.; Luo, X. Theoretical Studies of MoS 2 and Phosphorene Drug Delivery for Antituberculosis Drugs. *J. Phys. Chem. C* **2020**, *124*, 8279–8287, doi:10.1021/acs.jpcc.0c01256.
21. Wang, J.; Wang, Z.; Cheng, Y.; Cao, L.; Bai, F.; Yue, S.; Xie, P.; Ma, J. Molybdenum Disulfide (MoS2): A Novel Activator of Peracetic Acid for the Degradation of Sulfonamide Antibiotics. *Water Research* **2021**, *201*, 117291, doi:10.1016/j.watres.2021.117291.
22. Liao, L.; Yang, L.; Zhao, G.; Zhou, H.; Cai, F.; Li, Y.; Wang, X.; Yu, F. Boosting pH-Universal Hydrogen Evolution of Molybdenum Disulfide Particles by Interfacial Engineering †. *Chin. J. Chem.* **2021**, *39*, 288–294, doi:10.1002/cjoc.202000487.
23. Liaqat, A.; Yin, Y.; Hussain, S.; Wen, W.; Wu, J.; Guo, Y.; Dang, C.; Ho, C.-H.; Liu, Z.; Yu, P.; et al. An All Two-Dimensional Vertical Heterostructure Graphene/CuInP 2 S 6 /MoS 2 for Negative Capacitance Field Effect Transistor. *Nanotechnology* **2022**, *33*, 125703, doi:10.1088/1361-6528/ac4063.
24. Vatalaro, M.; De Rose, R.; Lanuzza, M.; Magnone, P.; Conti, S.; Iannaccone, G.; Crupi, F. Assessment of Paper-Based MoS2 FET for Physically Unclonable Functions. *Solid-State Electronics* **2022**, *194*, 108391, doi:10.1016/j.sse.2022.108391.
25. Espejo, C.; Rangel, T.; Romero, A.H.; Gonze, X.; Rignanese, G.-M. Band Structure Tunability in MoS 2 under Interlayer Compression: A DFT and GW Study. *Phys. Rev. B* **2013**, *87*, 245114, doi:10.1103/PhysRevB.87.245114.
26. Zhou, W.; Zou, X.; Najmaei, S.; Liu, Z.; Shi, Y.; Kong, J.; Lou, J.; Ajayan, P.M.; Yakobson, B.I.; Idrobo, J.-C. Intrinsic Structural Defects in Monolayer Molybdenum Disulfide. *Nano Lett.* **2013**, *13*, 2615–2622, doi:10.1021/nl4007479.
27. Giannozzi, P.; Baroni, S.; Bonini, N.; Calandra, M.; Car, R.; Cavazzoni, C.; Ceresoli, D.; Chiarotti, G.L.; Cococcioni, M.; Dabo, I.; et al. QUANTUM ESPRESSO: A Modular and Open-Source Software Project for Quantum Simulations of Materials. *J. Phys.: Condens. Matter* **2009**, *21*, 395502, doi:10.1088/0953-8984/21/39/395502.
28. Giannozzi, P.; Andreussi, O.; Brumme, T.; Bunau, O.; Buongiorno Nardelli, M.; Calandra, M.; Car, R.; Cavazzoni, C.; Ceresoli, D.; Cococcioni, M.; et al. Advanced Capabilities for Materials Modelling with Quantum ESPRESSO. *J. Phys.: Condens. Matter* **2017**, *29*, 465901, doi:10.1088/1361-648X/aa8f79.
29. Blöchl, P.E. Projector Augmented-Wave Method. *Phys. Rev. B* **1994**, *50*, 17953–17979, doi:10.1103/PhysRevB.50.17953.
30. Frenkel, D.; Smit, B. *Understanding Molecular Simulation: From Algorithms to Applications*; Computational science series; 2nd ed.; Academic Press: San Diego, 2002; ISBN 978-0-12-267351-1.
31. Marx, D.; Hutter, J. Ab Initio Molecular Dynamics: Theory and Implementation. In *Modern Methods and Algorithms of Quantum Chemistry, Proceedings*; Grotendorst, J., Ed.; NIC Series; John von Neumann Institute for Computing, 2000; Vol. 3, pp. 329–477 ISBN 3-00-005834-6.

32. Marx, D.; Hutter, J. *Ab Initio Molecular Dynamics: Basic Theory and Advanced Methods*; First paperback edition.; Cambridge University Press: Cambridge, 2012; ISBN 978-1-107-66353-4.
33. Lee, J.G. *Computational Materials Science: An Introduction*; Second edition.; CRC Press, Taylor & Francis Group, CRC Press is an imprint or the Taylor & Francis Group, an informa business: Boca Raton, 2017; ISBN 978-1-4987-4973-2.
34. Monkhorst, H.J.; Pack, J.D. Special Points for Brillouin-Zone Integrations. *Phys. Rev. B* **1976**, *13*, 5188–5192, doi:10.1103/PhysRevB.13.5188.
35. Kokalj, A. XCrySDen—a New Program for Displaying Crystalline Structures and Electron Densities. *Journal of Molecular Graphics and Modelling* **1999**, *17*, 176–179, doi:10.1016/S1093-3263(99)00028-5.
36. *Kramers-Kronig Relations in Optical Materials Research*; Lucarini, V., Ed.; Springer series in optical sciences; Springer: Berlin ; New York, 2005; ISBN 978-3-540-23673-3.
37. Jiménez-González, A.F.; Ramírez-de-Arellano, J.M.; Magaña, L.F. Substantial Variations in the Optical Absorption and Reflectivity of Graphene When the Concentrations of Vacancies and Doping with Fluorine, Nitrogen, and Oxygen Change. *International Journal of Molecular Sciences* **2021**, *22*, 6832, doi:10.3390/ijms22136832.
38. *Surface Science: An Introduction*; Oura, K., Ed.; Advanced texts in physics; Springer: Berlin ; New York, 2003; ISBN 978-3-540-00545-2.